Published in final edited form as:
J Ultrasound Med. 2008 December ; 27(12): 1699–1709.

A Method for Assessing the Microvasculature in a Murine Tumor Model Using Contrast-Enhanced Ultrasonography

Mary E. Loveless, MS, **Xia Li, PhD**, **Jessica Huamani, MS**, **Andrej Lyshchik, MD, PhD**, **Benoit Dawant, PhD**, **Dennis Hallahan, MD**, **John C. Gore, PhD**, and **Thomas E. Yankeelov, PhD**
from the Institute of Imaging Science (M.E.L., X.L., B.D., J.C.G., T.E.Y.) and Departments of Biomedical Engineering (M.E.L., D.H., J.C.G., T.E.Y.), Electrical Engineering and Computer Science (X.L., B.D.), Radiation Oncology (J.H., D.H.), Radiology and Radiological Sciences (A.L., J.C.G., T.E.Y.), Physics and Astronomy (J.C.G., T.E.Y.), and Cancer Biology (T.E.Y.), Vanderbilt University, Nashville, Tennessee USA.

Abstract

Objective—The purpose of this study was to develop a method for assessing tumor vascularity in a preclinical model of breast cancer using contrast-enhanced ultrasonography.

Methods—Eight mice were injected with 67NR breast cancer cells on their hind limbs and imaged with ultrasonography 8 days later. Mice were injected with an ultrasound contrast agent (UCA), and a sequence of images of the resultant backscattered echoes was recorded before and after high-power "destruction" pulses for each of multiple parallel planes. From these, data maps of the maximum contrast enhancement (within each time course) were constructed for each pixel, which enabled reconstruction of high-resolution coregistered sections into a 3-dimensional (3D) volume reflecting tumor vascularity. Additional studies were performed to determine the duration and repeatability of image enhancement, and images were correlated with conventional 3D power Doppler measurements.

Results—The lifetime of the UCA in vivo was found to be 4.3 ± 1.09 minutes (mean ± SD). The 3D contrast-enhanced ultrasonographic technique produced images that correlated well with power Doppler images in specific regions but also depicted additional regions of flow surrounding the power Doppler signal. The mean correlation coefficient between voxel measurements of the central slice for each animal was 0.64 ± 0.07 ($P < .01$). In addition, sequential studies in each animal were reproducible.

Conclusions—A method producing high-resolution volumetric assessments of tumor vascularity in a preclinical model of breast cancer is shown that correlates with other ultrasonographic measures of blood flow, which may provide greater sensitivity to the microvasculature.

Keywords

contrast-enhanced ultrasonography; tumor; vascularity

For a tumor to grow beyond approximately 1 to 2 mm^3, it cannot rely on the diffusion of metabolites and therefore must recruit and develop new vessels through the well-known process of angiogenesis. [1] Secretion of multiple growth factors from the tumor causes a chemotactic response from endothelial cells, which then migrate to the site to form vessels. Typically, the neovasculature arising from this process exhibits different characteristics from

Address correspondence to Thomas E. Yankeelov, PhD, Institute of Imaging Science, Vanderbilt University Medical Center, 1161 21st Ave S, MCN AA-1105, Nashville, TN 37232-2675 USA. E-mail: thomas.yankeelov@vanderbilt.edu.

the normal vasculature; the vessels are tortuous, leaky, and heterogeneously distributed within the tumor site.[2,3] In many types of cancer, a positive correlation between vascularity and invasiveness has been shown.[3] Some anticancer drugs specifically target angiogenesis to slow or stop the growth and invasion of the tumor by interfering with signaling pathways such as those mediated by members of the vascular endothelial growth factor family.[4] Several antiangiogenic drugs approved by the US Food and Drug Administration are used clinically, whereas others are under development.[5] Methods for assessing the vascular properties of tissues are of interest so that the efficacy of such drugs can be evaluated in a noninvasive way.

Ultrasound contrast agents (UCAs) are composed of small volumes of air or gas surrounded by a stabilizing shell that remain completely intravascular, making them ideal agents for vessel imaging.[6–10] Ultrasound contrast agents reflect sound strongly because they have a very different acoustic impedance from that of blood. In the presence of a sound field, the UCA begins to expand and contract. At a low input wave pressure (<50 kPa), the microbubbles behave as simple monopole oscillators, but at a higher input pressure (50–100 kPa), they may have nonlinear behavior, producing harmonics of the incident sound. At an even higher pressure (500 kPa–1MPa), the bubbles can be destroyed by extreme expansion and contraction, which can be advantageous in some applications.[11]

The aim of this study was to create high-resolution 3-dimensional (3D) depictions of tumor vascularity in small-animal cancer models. To develop this protocol, we performed additional studies to characterize the maximum enhancement time of the UCA at injection and how many destruction pulses could be administered while maintaining significant contrast enhancement. By applying the results of these studies, we propose an approach in which sequential acquisitions of multiplanar images after administration of a UCA can be registered and processed to provide images of the tumor vasculature.

Materials and Methods

Data Acquisition

Duration of UCA Enhancement—All procedures adhered to our institution's Animal Care and Use Committee guidelines. Eight female nude athymic (*nu/nu*) mice were injected subcutaneously with 10^6 67NR breast cancer cells[12] in the hind limb. The tumors were allowed to grow to approximately 8 to 10 mm in diameter, which typically occurred 8 days later. Twenty-six-gauge jugular catheters were surgically implanted for delivery of the contrast agent. This procedure was performed 2 days before imaging to allow the animals to fully recover. The mice were imaged on a Vevo 770 system (VisualSonics Inc, Toronto, Ontario, Canada) using a 40-MHz transducer mounted to a 3D motor on a rail system. During the imaging session, the animals were anesthetized with a 2%/98% isoflurane/oxygen mixture, and the body temperature was monitored and maintained at 37°C by a warming plate. The heart rate was also monitored and remained approximately 350 to 400 beats per minute.

Coupling gel was applied to the area of interest, and 2-dimensional (2D) B-mode and power Doppler scout images established a field of view with vascularity present. The field of view varied from 9 × 9 to 12 × 12 mm depending on the tumor size, and the acquisition matrix was 544 × 488, thereby establishing an in-plane pixel size of approximately 25 × 25 μm or less. Image acquisition began immediately before a 50-μL bolus of the VisualSonics MicroMarker UCA (1.0×10^8 microbubbles/50-μL injection) was injected via a jugular catheter. This UCA is specifically designed for high-frequency (30- to 45-MHz) ultrasound imaging, and the diameter of the microbubbles ranges from 2.3 to 2.9 μm. The MicroMarker UCA, developed with characteristics similar to those of the second-generation contrast agent SonoVue (Bracco SpA, Milan, Italy), is composed of a phospholipids shell containing perfluorobutane (product literature). Images were obtained in the VisualSonics contrast mode at a frame rate of 6 to 8

frames per second and 50% power (mechanical index, 0.14) for 10 minutes with no respiratory gating. This process was repeated (totaling 2 injections for each mouse) after 30 minutes, which allowed for clearance of any residual contrast.[13] This study provided information on the duration of useful contrast enhancement.

Vascular Enhancement Repeatability—Animal preparation and the field of view were identical to those in the duration of UCA enhancement study described above. Once the 50-μL bolus of the MicroMarker UCA reached equilibrium (≈45 seconds),[14,15] imaging began in the VisualSonics contrast mode at a frame rate of 14 frames per second and 50% power. In these studies, equilibrium was defined as a pseudo steady state of the UCA in the bloodstream, established by allowing an allotted time after injection to pass so the UCA became well mixed in the bloodstream. The time suggested by the literature[14,15] to allow the UCA to reach this equilibrium was confirmed by the study described above; by examination of the time-intensity curves (TICs), enhancement reached a plateau at approximately 45 seconds. A high-power ultrasound destruction sequence was then applied (20 cycles with a frequency of 10 MHz and a mechanical index of 0.59), and images were collected for approximately 15 to 20 seconds to assess enhancement. Twelve to eighteen sets of destruction/reperfusion images were collected over the maximum time dictated by the duration of the UCA enhancement study described above. This process was then repeated for each mouse after a 30-minute period to allow for elimination of the UCA from the blood. These data provided information on the repeatability of characterizing vascular enhancement in each animal.

Three-Dimensional Contrast-Enhanced Vascular Imaging—With a preparation identical to that described in the 2 studies above, B-mode scout images established the most posterior imaging plane of the region of interest (ROI). A 50-μL bolus of the UCA was injected and allowed to reach equilibrium within the blood pool. Imaging at 50% power began after equilibrium was reached, and a destruction pulse was administered, followed by 15 to 20 seconds of image acquisition with no respiratory gating. Images were obtained in the VisualSonics contrast mode at a frame rate of 14 frames per second. The transducer was calibrated to fix on the next region of tissue 330 μm in the anterior direction by manually incrementing a translation stage. A destruction pulse was administered, followed by another 15 to 20 seconds of image acquisition. This process was repeated for each slice of tissue until the entire tumor was covered. To maintain significant levels of enhancement as dictated by the vascular enhancement repeatability study described above, additional (up to 3) injections of the UCA were used to obtain vascular images of the entire tumor volume.

Three-dimensional power Doppler images were also obtained to compare the proposed vascular imaging method with an accepted ultrasonographic method for assessing flow. With the same field of view and step size as for the contrast-enhanced vascular imaging (CEVI) technique, 3D power Doppler and B-mode images of the tumor were also collected. As per the manufacturer's recommendation for optimally imaging the tumor vasculature, respiratory gating was used, and the power was set to 100%, with the scan speed and wall filter set to 2 and 2.5 mm/s, respectively.

Data Analyses

Duration of UCA Enhancement—Data analyses were performed with VisualSonics software, Excel 2003 (Microsoft Corporation, Redmond, WA), and MATLAB R2006a (The MathWorks, Natick, MA). An ROI was manually drawn around the entire tumor area, and the average intensity for each frame was computed to construct a TIC for each mouse. Time course images were obtained for each injection at an in-plane pixel size of approximately 25 × 25 μm. Regions of interest were drawn, and TICs were analyzed in this native resolution. Plots of the TICs were computed in Excel, and visual inspection was used to predict the maximum

clearance time of the UCA for the vascular enhancement repeatability study. Eight sets (each set consisting of 2 injections, 1 set per animal) of TICs were exported to Excel, and the minimum intensity value was subtracted from all points in the time course to eliminate the relative baseline signal. The relative baseline represents the minimum signal intensity immediately before a UCA injection or after the administration of a destruction pulse. For each set, the TIC obtained from the first injection was plotted against the second injection TIC, and a linear regression analysis was performed. Data were also analyzed by the Spearman rank correlation test to assess the strength of consistency for multiple injections. Additionally, each TIC was exported to MATLAB to determine the time during wash-out in which enhancement from the UCA fell below a 20% increase over the relative baseline during imaging. This parameter was used to determine the maximum useful time the UCA remained in circulation under a low input pressure.

Vascular Enhancement Repeatability—Again, data analyses were performed with VisualSonics software, Excel 2003, and MATLAB R2006a. Regions of interest of the entire tumor area were manually drawn, and the average intensity for each frame was computed to form a TIC for each subject. The data were then exported to MATLAB. Each data segment containing a destruction pulse and subsequent reperfusion frames was separated into individual files, and the minimum intensity value was subtracted from all points in the time course. Time course data were smoothed temporally by using a moving average filter with a window size of 3. This moving average filter replaces 3 adjacent points with an average of the replaced points, thereby smoothing the shape of the curve. This smoothing was performed to improve the signal-to-noise ratio.[16] Each time course for an injection contained 12 to 18 destruction/reperfusion segments. The number of destruction cycles before the maximum enhancement fell below 20% of the baseline was evaluated for each injection.

Three-Dimensional CEVI—Data analyses were performed with MATLAB R2006a, and Figure 1 illustrates the data-processing steps described below. The maximum duration for UCA image enhancement and the number of destruction pulses allowed before enhancement was no longer significantly above the baseline were determined from the 2 studies described above, and the results were applied to determine the protocol for 3D CEVI. A signal intensity was defined as significantly enhanced if the intensity was 20% or higher than the relative baseline. The video intensity data, without any additional compression (contrast or gray scale) curves, were then exported to MATLAB, and each frame within a time course was down sampled to a 256 × 256 image matrix. Frames within a data set were coregistered to other time course frames with a rigid-body algorithm to reduce any motion artifacts.[17,18] The registration algorithm relies on mutual information shared between each image set. A transformation is applied to the reference image, which maximizes shared information with the target image file. A number of postprocessing steps were performed to improve the signal-to-noise ratio.[16] The registered images were processed with a maximum intensity projection (MIP) algorithm. The last slice was subtracted from the relative baseline image, and any pixel displaying intensity of less than 20% of the maximum was eliminated (ie, set to 0 intensity). In addition, a maximum change in the intensity map was computed. The mean and SD were found from an ROI containing rapidly enhancing voxels, which are characteristic of the presence of a UCA. Any voxel below the mean of the ROI minus 1 SD was not considered rapidly enhancing and was set to 0 intensity. This threshold was chosen to optimize the reduction in the background while still preserving signal intensity from the UCA because there did exist some overlap between the background and contrast-enhanced signal in the B-mode images. Finally, the images were filtered for pixels that had fewer than 3 enhancing pixels surrounding the pixel being interrogated. The process was repeated for each slice within a volume.

Processed CEVI slices and anatomic slices were fused into separate volume images. Anatomic volumes from the 3D CEVI method were coregistered by the same registration approach as

above to anatomic volumes collected via the 3D B-mode. The transformation was also applied to the 3D power Doppler data, thereby registering it with the 3D contrast-enhanced data. Logical masks, where 1 represented a vasculature signal and 0 represented no vasculature signal, were created for both the contrast-enhanced slice and the corresponding power Doppler slice in all data sets. Two-dimensional Pearson correlation coefficients for each slice were calculated to test for a correlation between the magnitude of the contrast-enhanced signal and the power Doppler signal across all coregistered voxels in the slice.

Results

Duration of UCA Enhancement

Table 1 presents the time each injection took to return to approximately 20% above the baseline level. The mean time of UCA image enhancement ± SD was found to be 4.3 ± 1.09 minutes.

Figure 2 shows the TIC from injection 1 plotted against the TIC from injection 2 for a typical animal. Data were cropped such that they included only the wash-out from each injection because possible variations in the injection rate may have introduced variability in the wash-in curves. Because data collection for these studies was performed during a pseudo steady-state period after UCA uptake, assessments of the uptake kinetics were not performed. Table 1 describes the slope and *r* values corresponding to a linear regression comparing the time course values from injections 1 and 2. *P* values for all sets of injections were computed by the Spearman rank test and found to be less than .01 in all cases.

Vascular Enhancement Repeatability

Results were obtained from 6 mice; data from 2 mice were discarded because of errors in UCA injection; however, all 8 mice were successfully used in the other 2 studies described. Example TICs resulting from this study are presented in Figure 3. The number of destruction cycles for which significant contrast enhancement was available are reported in Table 2. The average number of destructions before the maximum enhancement fell below 20% of the baseline was 4 ± 2 pulses. These results were used to obtain vessel images in the subsequent study that had significant enhancement from the contrast agent and minimum background noise.

Three-Dimensional CEVI

Correlation coefficients for all slices within each animal were calculated, and the central slice, minimum, and maximum correlation coefficients for each animal are listed in Table 3. These correlation coefficients reflect the correlation between the magnitudes of the signals from the contrast-enhanced and power Doppler measurements for each voxel in each slice. The results in Table 3 confirm that the spatial maps of these 2 different measurements of vascular properties correlated well. For example, the mean *r* value of the central slice for each animal was 0.64 ± 0.07 ($P < .01$). By following the steps illustrated in Figure 1, Figure 4 shows the central imaging plane of 3 representative mice at different stages of CEVI development. Figure 4, a, e, and i, shows the B-mode images acquired before the UCA injection; and Figure 4, b, f, and j, displays the MIP images for the 3 subjects after the UCA was injected. Although the effects of blood flow are visualized in these images, the filtering algorithms described above clearly render vascular effects more completely, as shown in the third column (Figure 4, c, g, and k). The corresponding power Doppler images are depicted in Figure 4, d, h, and l, for comparison purposes. Figure 5, a, c, and e, shows 3D volumes of the tumor vasculature constructed in parallel planes. When corresponding fields of view were registered and examined, such as in Figure 6, higher distributions of the UCA seemed to dominate the areas surrounding the vasculature mapped by the power Doppler technique. Furthermore, the contrast-enhanced data appear to reveal areas of increased blood volume that were not detected by the power Doppler method. This phenomenon was not unexpected because contrast-enhanced ultrasonography is

known to be more sensitive than power Doppler imaging to microvasculature at the capillary level.[19]

Discussion

There are several imaging methods, including computed tomography, magnetic resonance imaging, and ultrasonography, that are available for assessing vascular properties. In most of these techniques, an exogenous contrast agent is used. Contrast-enhanced computed tomography using intravascular contrast agents has been used to assess blood flow and small vessels but cannot be used repeatedly because of considerations of x-ray exposure. Magnetic resonance methods have been adopted to be able to depict major vessels (magnetic resonance angiography) and blood volume and flow. Although magnetic resonance angiography in small animals can resolve intratumoral vessels at approximately 100μm, high-resolution images come at the expense of time and cost.[20] In addition, bulk out-of-plane motion during the long scan is difficult to correct. In ultrasonography, Doppler methods have also been able to detect microvessels on the scale of 30 to 100 μm.[21,22] Even with Doppler ultrasonographic techniques offering such high vessel resolution, detecting slowly flowing blood is difficult because of filters required to discriminate flow from vessel wall motion as well as heart and breathing motion.[23]

Ultrasound contrast agents have improved on ultrasonographic angiography techniques.[24] Harmonic imaging[25] is a method that detects only frequencies at approximately double the transmitted frequency; thus, the second harmonic of the resonating UCA is detected, whereas most echoes from the tissue are removed in a filtering process. However, because of the reduced bandwidth from filtering, the spatial resolution of the image is reduced depending on the frequency of the transmission signal, which was detailed by Goertz et al.[26] Another contrast-specific imagine technique is pulse inversion imaging. By applying an inverted pulse immediately after the primary pulse, the sum of linear echoes received from tissue will equal 0, whereas the nonlinearly resonating UCA will produce a summed echo greater than 0. Because there are no bandwidth restrictions with this technique, pulse inversion does not suffer from reduced image resolution. Both harmonic imaging and pulse inversion imaging can be used in conjunction with Doppler imaging to improve image quality.[27] Studies have shown that using these contrast-specific techniques in conjunction with Doppler imaging has improved tissue echo suppression and flow detection.[28,29]

Although harmonic and pulse inversion imaging techniques have improved noise suppression, there still remain limitations with these techniques using high-frequency scanning. Several in vivo studies have indicated the possibility of using UCAs with high-frequency systems to enhance detection of the vasculature.[30,31] Recently, Goertz et al[26,32] showed the feasibility of nonlinear high-frequency imaging with UCAs, but this approach requires extensive hardware modifications to detect the nonlinear characteristics of the UCAs, and commercialization of these prototypes is still under development.

The goal of this study was to develop and evaluate a straightforward method for obtaining high-resolution 3D images of the tumor vasculature on ultrasound scanners that can acquire 3D B-mode images. To establish the technique presented here, the characteristics of the UCA enhancement patterns and kinetics were studied to develop a protocol involving repeated destruction sequences. This lifetime is highly relevant to the design of imaging studies involving UCAs to assess vascular properties. With a fixed and moderate power level, the wash-out curves appear reasonably consistent when repeated. The vascular enhancement repeatability study was also useful for providing data from which a 3D technique could be designed. With each administered destruction pulse, a fraction of the injected UCA is destroyed from circulation. This study showed that the sequence of destruction followed by wash-in of

the UCA could be reliably repeated on average 4 times per injection. This is dependent not only on how long the UCA remains in circulation but also on the rate at which new bubbles enter and exit each region (ie, flow).

On visual inspection of the curves produced during the vascular enhancement repeatability study, most data sets showed a slow decline of contrast enhancement, but some data sets appeared to lose a significant percentage of enhancement after the first pulse. This observation could be the result of the number and distribution of vessels within the tissue in the imaging plane. If a section of tissue was highly vascularized, a larger amount of the contrast could have been destroyed, thereby reducing subsequent enhancement of the tumor region. Another reason could be that the UCA did not reach a steady state in the bloodstream. Care was taken to ensure that a pulse was not delivered until 45 seconds after injection, but if the UCA had not fully dispersed or the rate of injection was varied, the destruction of a large bolus could have affected the maximum number of pulses allotted to a volume of data.

The results of the 3D technique presented here show potential for using this technique for future studies of tumor vasculature. Although there does exist a correlation between the contrast-enhanced and power Doppler methods, a strong correlation was not necessarily expected between the 2 methods for several reasons. In Figure 6, the first arrow shows an example of a region detected by both methods. However, the second and third arrows depict the increased sensitivity of the contrast-enhanced method over the power Doppler method. As shown by the second arrow, the contrast-enhanced method had greater sensitivity to the microvasculature of areas surrounding the primary vessels detected by the power Doppler method; this attribute has been noticed in previous reports.[19,33] The third arrow points out that the contrast-enhanced technique even has the capability to detect vessels that are occult on power Doppler imaging. Although this finding needs to be confirmed by histologic studies, it suggests that the power Doppler technique underestimates the extent of the vasculature, whereas UCAs appear to be more sensitive to the vasculature neglected by the power Doppler measurement.

Although this work shows promising preliminary results, limitations in this study require future work. First, the UCA was delivered manually in all of the studies discussed above. To optimize repeatability of any of these studies and minimize human error, an automated syringe pump should be used. With an automated syringe pump, both the amount of the UCA injected as well as the rate of injection are controlled across multiple injections and multiple subjects.

Reducing subject motion is imperative when using high-resolution scanners. Although intraslice registration aided in eliminating motion artifacts, additional filters were needed to further isolate the UCA from artifacts produced from motion or speckles. Although these filters isolate the UCA by exploiting the properties of the UCA, refinement of the methods of isolating the ultrasound contrast signal is necessary to provide more quantifiable results. Development of a more sophisticated tracking algorithm based on the temporal and spatial location of the UCA may provide very specific borders within the microvasculature.

Automated rigid registration between the final volume sets provided a voxel-by-voxel comparison of the 2 data sets. However, interpolation between slices as well as errors during manual incremental stepping in the contrast-enhanced technique required adjustment of initial parameters, making the applied registration semiautomated. The use of a motor with a fixed step size in future studies would aid in eliminating registration issues due to errors in stepping between slices.

The 3D contrast-enhanced ultrasonographic approach presented here not only preserves the characteristic advantages of speed and accessibility associated with ultrasound but also provides a method for creating high-resolution 3D images of tumor vessels. By this merit, the

method could offer an imaging alternative for studying the efficacy of, for example, antiangiogenic drugs on the tumor vasculature status in preclinical models.

Abbreviations

CEVI, contrast-enhanced vascular imaging; MIP, maximum intensity projection; ROI, region of interest; TIC, time-intensity curve; 3D, 3-dimensional; 2D, 2-dimensional; UCA, ultrasound contrast agent.

Acknowledgements

We thank Jarrod True, MS, for assistance with animal handling and Tuhin Sinha, PhD, and Jeff Luci, PhD, for technical assistance. This work was supported by the American Institute of Ultrasound in Medicine Endowment for Education and Research, National Institutes of Health grant 5 T32 EB003817, and National Cancer Institute Small Animal Imaging Resource Program Grant U24 CA126588. Dr Yankeelov was supported by National Institute of Biomedical Imaging and Bioengineering (NIBIB) grant 1K25 EB005936-01. Dr Li was supported by NIBIB grant 2R01 EB000214-15A1.

References

1. Folkman J. Anti-angiogenesis: new concept for therapy of solid tumors. Ann Surg 1972;175:409–416. [PubMed: 5077799]
2. Jain RK. Determinants of tumor blood flow: a review. Cancer Res 1988;48:2641–2658. [PubMed: 3282647]
3. Weidner N, Semple JP, Welch WR, Folkman J. Tumor angiogenesis and metastasis: correlation in invasive breast carcinoma. N Engl J Med 1991;324:1–8. [PubMed: 1701519]
4. Ferrara N, Kerbel RS. Angiogenesis as a therapeutic target. Nature 2005;438:967–974. [PubMed: 16355214]
5. Red-Horse K, Ferrara N. Imaging tumor angiogenesis. J Clin Invest 2006;116:2585–2587. [PubMed: 17016553]
6. Schlief R. Development in echo-enhancing agents. Clin Radiol 1996;51:5–7. [PubMed: 8605773]
7. Ayida G, Harris P, Kennedy S, Seif M, Barlow D, Chamberlain P. Hysterosalpingo-contrast sonography (HyCoSy) using Echovist-200 in the outpatient investigation of infertility patients. Br J Radiol 1996;69:910–913. [PubMed: 9038525]
8. Quay SC. Ultrasound contrast agent development: phase shift colloids [abstract]. J Ultrasound Med 1994;13:S9.
9. Schneider M, Arditi M, Barrau MB, et al. BR1: a new ultrasonographic contrast agent based on sulfur hexachloride-filled microbubbles. Invest Radiol 1995;30:451–457. [PubMed: 8557510]
10. Bauer, A.; Mahler, M.; Urbank, A. Microvascular imaging: results from a phase 1 study of the novel polymeric contrast agent SHU 563 A. In: Nanda, N.; Schlief, R.; Goldberg, B., editors. Advances in Echo Imaging Using Contrast Enhancement. Vol. 2nd ed. Lancaster, England: Kluwer Academic Publishers; 1997. p. 39-64.
11. Burns PN, Wilson SR. Microbubble contrast for radiological imaging, 1: principles. Ultrasound Q 2006;22:5–13. [PubMed: 16641788]
12. Aslakson CJ, Miller FR. Selective events in the metastatic process defined by analysis of the sequential dissemination of subpopulations of a mouse mammary tumor. Cancer Res 1992;52:1399–1405. [PubMed: 1540948]
13. Lindner JR, Dayton PA, Coggins MP, et al. Noninvasive imaging of inflammation by ultrasound detection of phagocytosed microbubbles. Circulation 2000;102:531–538. [PubMed: 10920065]
14. Wei K, Jayaweera AR, Firoozan S, Linka A, Skyba DM, Kaul S. Quantification of myocardial blood flow with ultrasound-induced destruction of microbubbles administered as a constant venous infusion. Circulation 1998;97:473–483. [PubMed: 9490243]
15. Lucidarme O, Kono Y, Corbeil J, et al. Angiogenesis: Noninvasive quantitative assessment with contrast-enhanced functional US in murine model. Radiology 2006;239:730–739. [PubMed: 16714458]

16. Yeh CK, Ferrara KW, Kruse DE. High-resolution functional vascular assessment with ultrasound. IEEE Trans Med Imaging 2004;23:1263–1275. [PubMed: 15493694]

17. Maes F, Collignon A, Vandermeulen D, Marchal G, Suetens P. Multimodality image registration by maximization of mutual information. IEEE Trans Med Imaging 1997;16:187–198. [PubMed: 9101328]

18. Li, R. Automatic Placement of Regions of Interest in Medical Images Using Image Registration [master's thesis]. Nashville, TN: Vanderbilt University; 2001.

19. Cosgrove D. Angiogenesis imaging: ultrasound. Br J Radiol 2003;76(special issue 1):S43–S49. [PubMed: 15456713]

20. Kobayashi H, Kawamoto S, Saga T, et al. Micro-MR angiography of normal and intratumoral vessels in mice using dedicated intravascular MR contrast agents with high generation of polyamidoamine dendrimer core: reference to pharmacokinetic properties of dendrimer-based MR contrast agents. J Magn Reson Imaging 2001;14:705–713. [PubMed: 11747027]

21. Goertz DE, Christopher DA, Yu JL, Kerbel RS, Burns PN, Foster FS. High-frequency color flow imaging of the microcirculation. Ultrasound Med Biol 2000;26:63–71. [PubMed: 10687794]

22. Goertz DE, Yu JL, Kerbel RS, Burns PN, Foster FS. High-frequency 3-D color-flow imaging of the microcirculation. Ultrasound Med Biol 2003;29:39–51. [PubMed: 12604116]

23. Wilson SR, Burns PN. Microbubble contrast for radiological imaging, 2: applications. Ultrasound Q 2006;22:15–18. [PubMed: 16641789]

24. Cosgrove D. Echo enhancers and ultrasound imaging. Eur J Radiol 1997;26:64–76. [PubMed: 9481589]

25. Burns PN, Powers JE, Fritzsch T. Harmonic imaging: a new imaging and Doppler method for contrast-enhanced ultrasound [abstract]. Radiology 1992;185:285.

26. Goertz DE, Cherin E, Needles A, et al. High frequency nonlinear B-scan imaging of microbubble contrast agents. IEEE Trans Ultrason Ferroelectr Freq Control 2005;52:65–79. [PubMed: 15742563]

27. Burns PN, Wilson SR, Hope-Simpson D. Pulse inversion imaging of liver blood flow: improved method for characterizing focal masses with microbubble contrast. Invest Radiol 2000;35:58–71. [PubMed: 10639037]

28. Burns PN, Powers JE, Hope-Simpson D, Uhlendorf V, Fritzsch T. Harmonic contrast-enhanced Doppler as a method for the elimination of clutter: in vivo duplex and color studies [abstract]. Radiology 1993;189:285. [PubMed: 8372207]

29. Hope-Simpson D, Chin CT, Burns PN. Pulse inversion Doppler: a new method for detecting nonlinear echoes from microbubble contrast agents. IEEE Trans Ultrason Ferroelectr Freq Control 1999;46:372–382. [PubMed: 18238434]

30. Deng CX, Lizzi FL, Silverman RH, Ursea R, Coleman DJ. Imaging and spectrum analysis of contrast agent in the in vivo rabbit eye using very-high-frequency ultrasound. Ultrasound Med Biol 1998;24:383–394. [PubMed: 9587993]

31. Kruse D, Lim MC, Redline DE, et al. High frequency ultrasound with an eigen-decomposition filter to assess the effect of laser cyclophotocoagulation treatment on blood flow. Proc IEEE Ultrason Symp 2002;2:1485–1489.

32. Goertz DE, Needles A, Burns PN, Foster FS. High-frequency, nonlinear flow imaging of microbubble contrast agents. IEEE Trans Ultrason Ferroelectr Freq Control 2005;52:495–502. [PubMed: 15857059]

33. Lagalla R, Caruso G, Urso R, Bizzini G, Marasà L, Miceli V. The correlation between color Doppler using a contrast medium and the neoangiogenesis of small prostatic carcinomas [in Italian]. Radiol Med (Torino) 2000;99:270–275. [PubMed: 10884828]

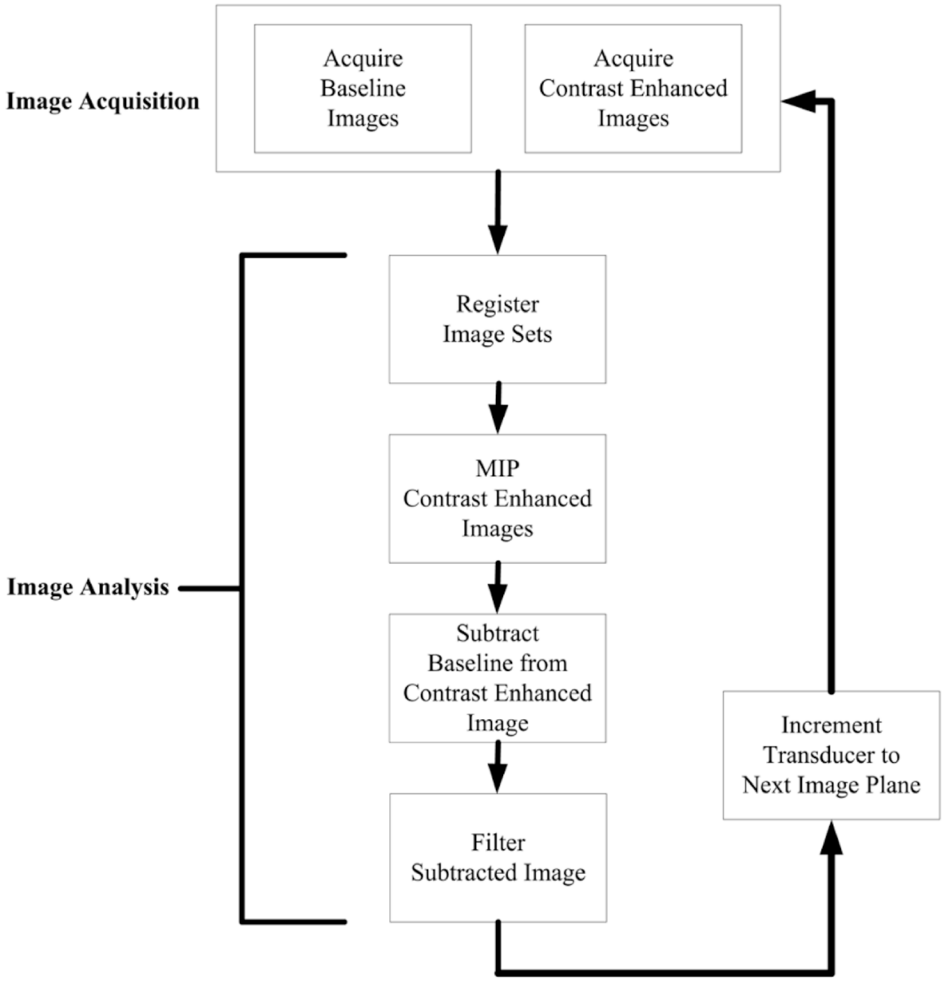

Figure 1.
Summary of data acquisition and analysis steps used in the development of 3D contrast-enhanced volumes.

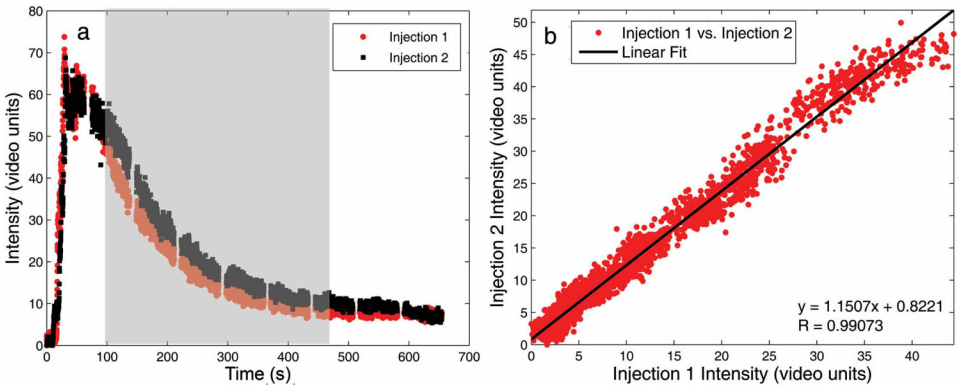

Figure 2.

a,Entire preinjection and postinjection TICs with the highlighted region that was compared in **b**. The linearity shown in **b** depicts consistent wash-out kinetics with multiple injections.

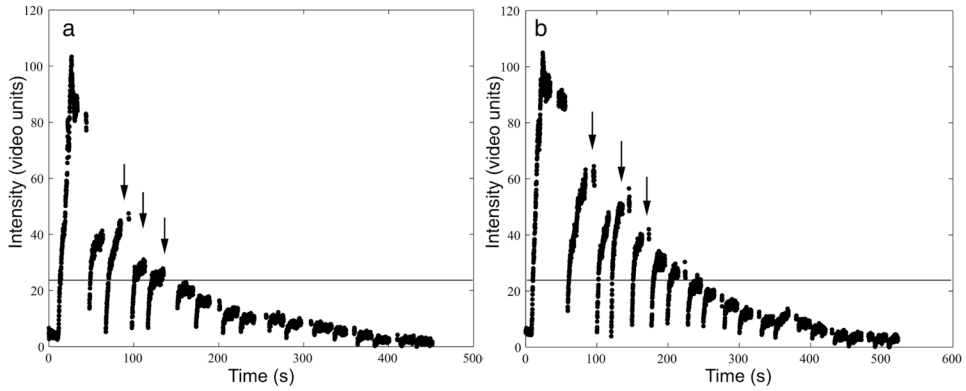

Figure 3.

Examples of multiple destructions applied to 1 slice of tissue. The arrows indicate several examples of the applied destruction pulse followed by the reperfusion of the UCA. The horizontal line indicates 20% above the baseline. After a destruction pulse is administered, the replenishment must rise above this baseline to be considered significantly enhancing.

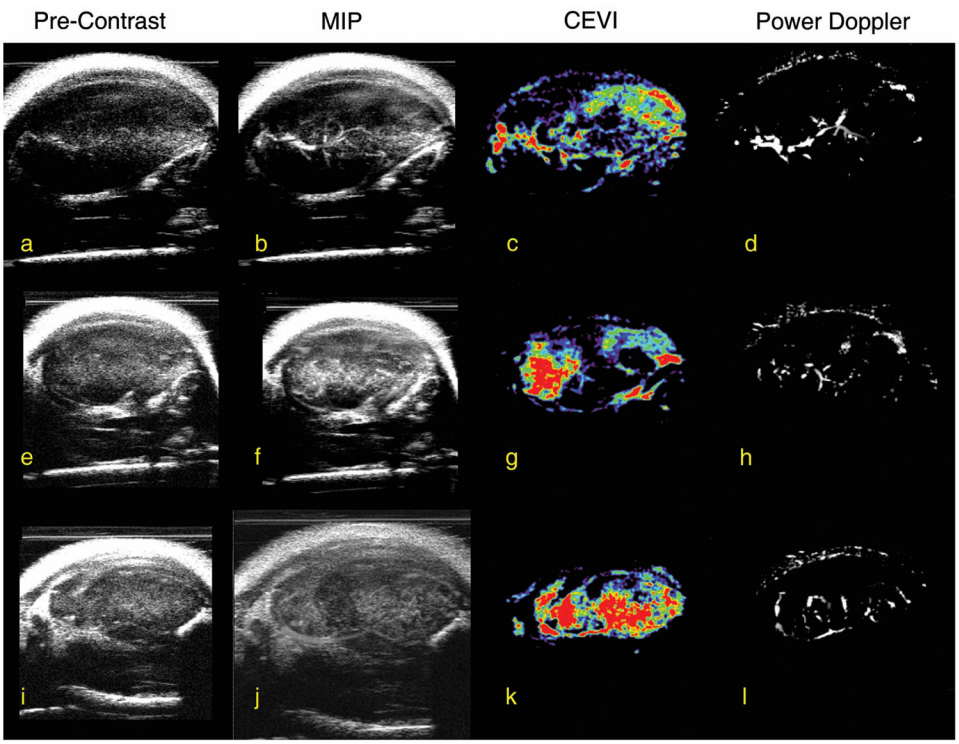

Figure 4.

Step-by-step overview of the UCA isolation technique for 3 mice. The first column (**a**, **e**, and **i**) depicts 2D B-mode images of the tumor before injection of any contrast agent, whereas the second column (**b**, **f**, and **j**) show the MIP image of the same section of tissue for each subject. After applying filters (see “Materials and Methods” for discussion of the filters) to isolate the UCA, images presented in the third column (**c**, **g**, and **k**) were constructed, and the power Doppler images in the fourth column (**d**, **h**, and **l**) for the same section of tissue are shown for comparison.

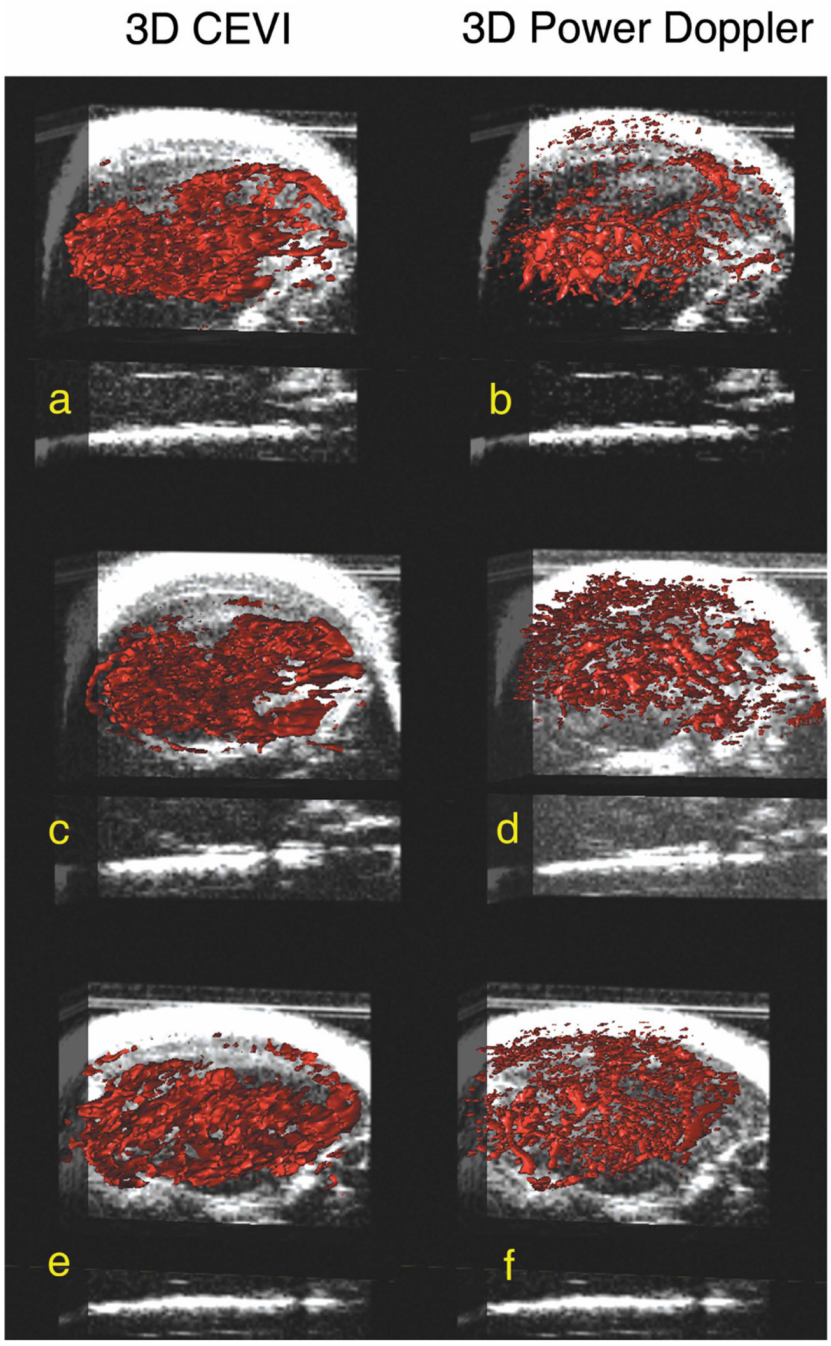

Figure 5.

Three-dimensional surface renderings of both the reconstructed 3D contrast-enhanced images (**a**, **c** and **e**) and 3D power Doppler images (**b**, **d**, and **f**) overlaid on slice-by-slice anatomic B-mode data. By applying the technique summarized in Figure 3 to all images in the tumor volume, the aligned images produced a 3D rendering of the sections of tissue, which showed significant enhancement due to the presence of intravascular microbubbles shown in **a**, **c**, and **e**.

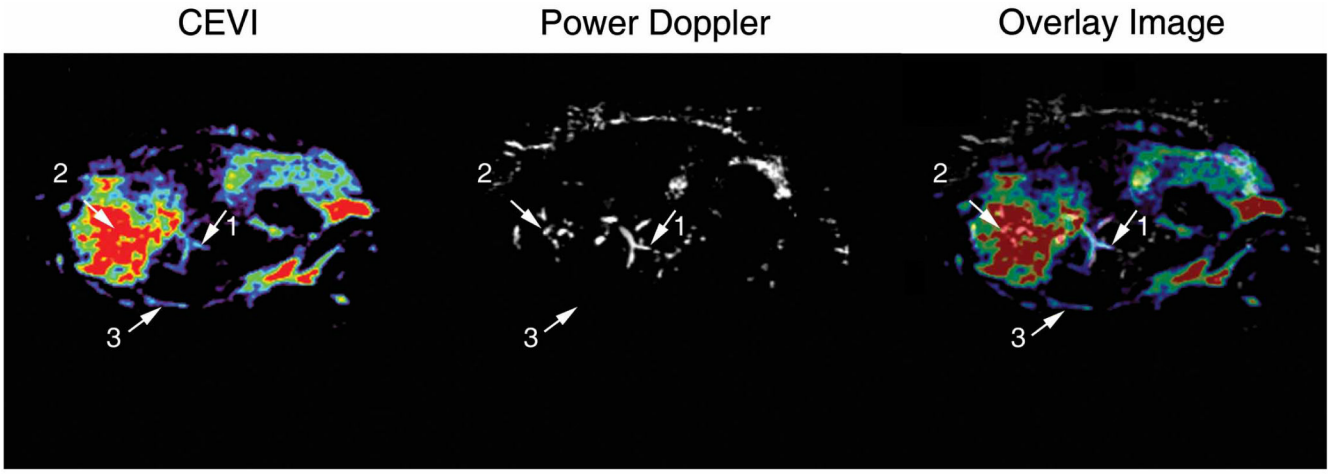

Figure 6.
Comparison of the contrast-enhanced and power Doppler techniques on a 2D image of the same section of tissue. Both the contrast-enhanced and power Doppler techniques were able to detect the bifurcating vessel indicated as reference point 1. However, the contrast-enhanced technique appeared to be more sensitive to the microvasculature surrounding the primary vessels detected at reference point 2. In addition, the contrast-enhanced technique detected the vessel located at reference point 3 that was otherwise missed by the power Doppler technique.

Table 1

Results From the Duration of UCA Enhancement Study

	Mouse															
Parameter	**1**		**2**		**3**		**4**		**5**		**6**		**7**		**8**	
Injection	1	2	1	2	1	2	1	2	1	2	1	2	1	2	1	2
Time, min	3.8	4.2	4.2	5.6	3.6	4.5	5.3	4.7	4.1	5.3	4.8	3.9	1.9	3.2	3.3	6.6
Slope	1.85		1.15		1.26		0.64		0.47		1.49		0.70		0.74	
r	0.97		0.99		0.92		0.66		0.95		0.99		0.69		0.96	
Spearman rank test *P*	<.01		<.01		<.01		<.01		<.01		<.01		<.01		<.01	

Table 2

Results From the Vascular Enhancement Repeatability Study

	Mouse															
Parameter	**1**		**2**		**3**		**4**		**5**		**6**		**7**		**8**	
Injection	1	2	1	2	1	2	1	2	1	2	1	2	2	2	1	2
Destruction pulses, n	4	7	4	7	NA	NA	NA	NA	7	6	1	2	2	4	5	4

NA indicates not applicable.

Table 3

Results From the CEVI and Power Doppler ROI Correlation

	Mouse							
Parameter	**1**	**2**	**3**	**4**	**5**	**6**	**7**	**8**
Central slice *r*	0.672	0.561	0.784	0.552	0.612	0.665	0.671	0.626
Maximum *r*	0.676	0.674	0.784	0.616	0.642	0.665	0.729	0.717
Minimum *r*	0.413	0.372	0.448	0.373	0.385	0.285	0.179	0.314
P	<.01	<.01	<.01	<.01	<.01	<.01	<.01	<.01